J Mol Model (2008) 14:651–658
DOI 10.1007/s00894-008-0295-y

ORIGINAL PAPER

# Elongation cutoff technique: low-order scaling SCF method

**Jacek Korchowiec · Jakub Lewandowski**

Received: 15 November 2007 / Accepted: 21 February 2008 / Published online: 2 April 2008


**Abstract** The elongation cutoff technique at restricted Hartree-Fock (HF) level of theory in conventional type of calculations, i.e., with two electron integrals (TEI) stored on a disc, is presented for two model systems. It is demonstrated that the number of TEI in the elongation cutoff calculations increases linearly with the system size thus, allowing to extend the conventional type of calculations to bigger systems. The step CPU (central processing unit) time in the elongation cutoff calculations is much lower than in the HF reference calculations. Such behavior reduces significantly the prefactor in the quadratic scaling relation. The total CPU time in the elongation calculation is about 40% lower than in the conventional HF calculations or comparable to direct type of calculations with the quantum fast multipoles method employed. It is shown that by introducing the interaction radius one can obtain linear scaling in the SCF calculations. *Figure:* The structure of density matrix and total CPU timings for polyglycine clusters in the elongation cutoff calculations.

**Keywords** Elongation cutoff technique · Elongation method · Fragmentation techniques · Linear scaling SCF calculations

## Introduction

There are two main approaches leading to linear scaling in quantum chemical calculations. On one side, new algorithms and formalisms are developed which linearize every step in Hartree-Fock (HF) and Kohn-Sham (KS) schemes [1–7], or diminish the scaling properties in the post-HF methods [8–15]. Here, the best example is the continuous fast multipole method [1, 2]. The second family of approaches to linear scaling problem constitutes the fragmentation techniques. These techniques are based on nearsightedness approximation. In other words, the electronic structure of a given part of a molecule is mainly determined by its nearest neighborhood and the very distant parts of the molecule have practically no effect on it. Two types of fragmentation techniques can be distinguished: the electron density based schemes [16–34] and energy based schemes [35–40]. The former schemes build the electron density of the whole system from subsystem densities while the latter compute the total energy or other quantities using the matching rules. The best example of density based approaches is divide-and-conquer of Yang [16, 17]. For a change, the fragment molecular orbital method of Kitaura [35, 36] is an example of energy based methods. The elongation cutoff method [18–23, 31–34] that is the subject of the paper belongs to density based approaches.

The elongation method was introduced in the 1990s by Imamura and Aoki [18, 19] in order to synthetize the electronic structure of aperiodic polymers. The method was adopted for KS and HF schemes at restricted, unrestricted and open-restricted levels of theory for both 'conventional' and 'direct' type of calculations [18–31, 32–34]. The method works within localized molecular orbital (MO) reference frame. The earliest version used two by two rotation to localize MOs. Therefore, the elongation method was practically not applicable to extended basis sets since the localization within the virtual subspace was too time consuming. Recently, we have introduced a localization scheme in which a few subsequent rotations are performed

J. Korchowiec (✉) · J. Lewandowski
K. Gumiński Department of Theoretical Chemistry,
Faculty of Chemistry, Jagiellonian University,
R. Ingardena 3,
30–060 Kraków, Poland
e-mail: Korchow@chemia.uj.edu.pl

on the whole density matrix [31]. This localization procedure is fast and reliable, thus removing the initial limitations of the elongation method. Later on, we have introduced a cut off technique to the elongation method [32–34]. This exact construction within the limit of perfect localization substantially reduces the number of computed two electron integrals (TEI), and therefore can significantly speed up the calculations.

In this paper we would like to demonstrate that the elongation cutoff technique extends the conventional type of HF calculations, with integrals stored on a disc, and the overall CPU (central processing unit) time of the elongation cutoff technique is lower than in the HF method. Two model systems are taken into account, namely, water chains and α-helix conformer of polyglycine. The former, weekly bound system guarantees that the total number of TEI is relatively small and the elongation cutoff technique can be directly compared to the conventional HF calculations. The later corresponds to strongly coupled subsystems and represents the most common secondary structure of proteins. The effect of basis set on accuracy and CPU time is discussed. The paper is organized as follows. First, we describe the elongation method. Then the cutoff procedure is explained. Next, we give information connected with computational details. After these sections, the test results are presented. Finally, the conclusions are given along with the future prospects.

## Elongation cutoff scheme

The elongation scheme [18, 19, 31, 34] mimics the polymerization/copolymerization reaction mechanism. Therefore, in the strict analogy to this reaction, the following steps in the elongation procedure can be distinguished:

$$M_1 \overset{SCF}{=} (A_1|B_1) \quad (initialization) \tag{1}$$

$$\begin{cases} M_2 = (A_1|B_1 + C_1) \equiv (A_1|S_1) \overset{SCF}{=} (A_1 + A_2|B_2) \equiv (A^2|B_2) \\ M_3 = (A^2|B_2 + C_2) \equiv (A^2|S_2) \overset{SCF}{=} (A^2 + A_3|B_3) \equiv (A^3|B_3) \\ \quad \vdots \\ M_{n-1} = (A^{n-2}|S_{n-2}) \overset{SCF}{=} (A^{n-2} + A_{n-1}|B_{n-1}) \equiv (A^{n-1}|B_{n-1}) \end{cases} \quad (propagation) \tag{2}$$

$$M_n = \left(A^{n-1}|B_{n-1} + C_{n-1}\right) \equiv \left(A^{n-1}|S_{n-1}\right) \quad (termination). \tag{3}$$

The HF calculations performed for a starting cluster $M_1$ followed by MOs localization into $A_1$ and $B_1$ regions initialize the elongation scheme [31]. The fragment $A_1$ is defined by atoms that are far away from the chain-propagation center. The remaining atoms belong to $B_1$. More precisely, the definition of the fragment extends to all its atomic orbitals (AOs). We associate the word "region" with the localized MO (LMO) basis, since it also contains contributions from other fragment. Only in the limit of perfect localization the definition of fragment is "equivalent" to that of the region.

In the first propagation step, MOs assigned to $A_1$ region are kept frozen while those assigned to $B_1$ region together with MOs of a monomer $C_1$ define the active space $S_1$. After solving HF equation, the active space MOs are localized into $A_2$ and $B_2$ regions. In the second propagation step, LMO assigned to frozen part $A_1+A_2 \equiv A^2$ are excluded from the variational space, and only those of $B_2$ and $C_2$ fragments compose the variational space $S_2$. Again, the convergence in the SCF process means that the active space MOs are localized into $A_3$ and $B_3$ regions. The remaining propagation steps look similarly, only the frozen part is getting bigger. In the case of polymerization reaction, the number of active space MOs is constant, while in the case of copolymerization reaction, it oscillates around the average value. In the final, termination step, the localization part can be omitted.

Apart from the LMO localization procedure, a central role in the elongation methods plays the transformation that narrows the variation space:

$$F^{MO}(S_i) \equiv (C_{S_i})^{\dagger} F\left(A^i|S_i\right) C_{S_i} \tag{4}$$

Here, $C_{S_i}$ is a rectangular matrix collecting active space MOs. It is a part of a full MO square matrix, $C_{M_{i+1}} = (C_{A^i}, C_{S_i}) = (C_{A_1}, C_{A_2}, \ldots, C_{A_i}, C_{S_i})$. The frozen MOs are excluded from the transformation, so the resultant square matrix, $F^{MO}(S_i)$, is of lower dimension (equal to the number of active space MOs). Then, the pseudo-eigenvalue problem is solved in a self-consistent way:

$$F^{MO}(S_i) C^{MO}_{S_i} = S^{MO} C^{MO}_{S_i} E_{S_i} \tag{5}$$

and $C^{MO}_{S_i}$; are transferred back to AO representation $C_{S_i}$.

The idea of cut-off technique [32–34] is very simple. Let us consider Eq. (4) for the first propagation step. In the limit of perfect localization, the frozen orbitals have no tailings in the active part and vice versa, the active orbitals have no tailings in the frozen region. In other words, some of the blocks in $C_{M_2}$ are filled with zeros (see Fig. 1). The zero block in the active $C_{S_1}$ simply cuts $F_{A_1A_1}$ and $F_{S_1A_1}$ blocks out when the entire AO Fock matrix is transformed. The only contribution that survived in the resultant matrix is $C^{\dagger}_{S_1S_1} F_{S_1S_1} C_{S_1S_1}$. Therefore, at this point we have clear-cut evidence that the construction of the full AO Fock matrix is simply a waste of time. Instead we can compute the $F_{S_1S_1}$ block only.

This very ideal situation never takes place. Therefore, we have to introduce a threshold value that reflects the

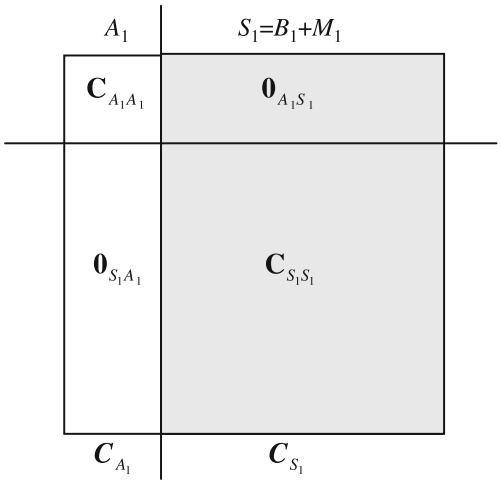


**Fig. 1** The structure of the MO matrix in the limit of perfect localization

effective coupling between a given subset of frozen and active orbitals. If the coupling is below the threshold we can disregard a given fragment in the next step. It does not mean that the interaction between the cut and remaining fragments are switched off. Therefore, the density matrix of the entire system (**D**') is required for constructing $F_{S_1S_1}$. Its cutoff part ($\mathbf{D}_{\text{cutoff}}$) is invariable in the current and subsequent steps. One should also notice that the cut MOs introduce a correction (δ**D**) to the current density matrix (**D**). If cutoff technique is applied to covalently bound systems then at least one bond is "broken", i.e., the corresponding LMO should be shifted either to cut or to current molecular fragment. In such a case, the calculations are performed for cation or anion. In the first case (δ**D**) is big because we give back an "electron" to the current system.

In practice, after at least two elongation steps we can perform the first cutoff step. In Fig. 2, we have shown a chart flow diagram for elongation cut-off SCF calculations. In this particular example, we have assumed that the condition for cutoff is fulfilled after three elongation steps. The initial density, being a direct sum of **D** and $\mathbf{D}_{\text{cutoff}}$, is utilized to construct the AO Fock matrix, $\mathbf{F}(A_2,A_3,A_4|B_4,C_4) \equiv \mathbf{F}$ (S'). It is worth mentioning here, that we are computing less TEI than in normal elongation or HF schemes and this difference is getting bigger and bigger with every subsequent cutoff step. Next, we diminish the dimension of the variational space by transforming the Fock AO matrix to MO representation as in normal elongation case. Then the HF equations are solved in the MO basis. The obtained MOs of the active space are transformed back to AO representation. The iteration loop is finished after calculating **D**. If the density is converged we finish the SCF process otherwise all steps are repeated. Finally, we localize $S_4$ into a new frozen part $A_5$ and a new active part $B_5$, and we

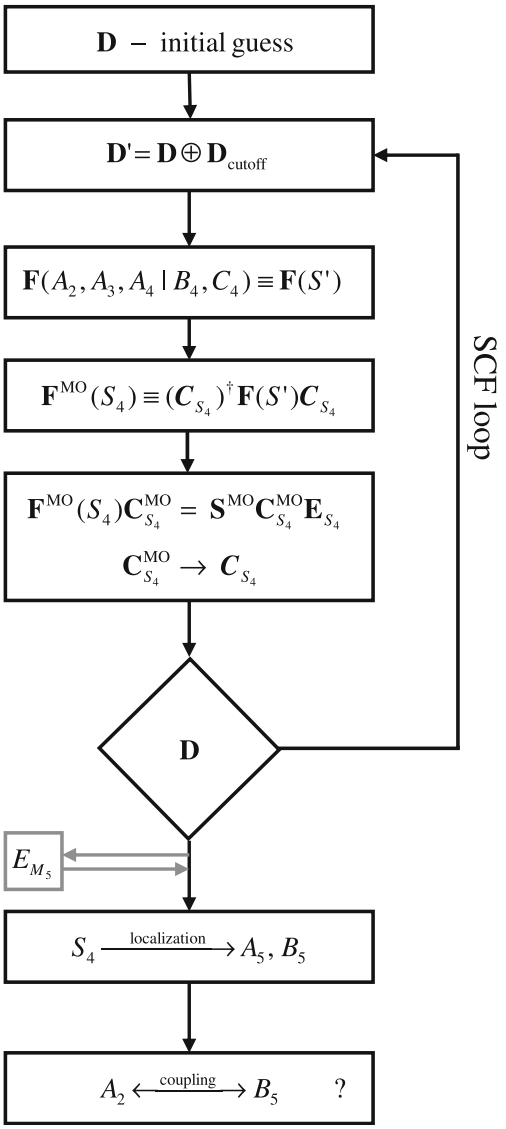


**Fig. 2** Flowchart for the elongation cutoff SCF scheme as applied for first cuttoff propagation step (performed after three normal elongation steps) of the elongation procedure. Matrices marked by MO superscript correspond to MO (LMO) basis, the remaining matrices correspond to AO basis

check the coupling between $A_2$ and $B_5$. If the coupling is again below the threshold value we can drop $A_2$ in the next elongation cutoff step. One can eventually compute the energy of the entire system, however, this can be postponed to the final elongation cutoff step.

## Computational details

The cutoff elongation scheme has been implemented and linked to the GAMESS program package [41, 42]. All calculations are performed at the HF level of theory. Two model systems, i.e., linear water chains and α-helix of polyglycine are taken into account. The translational

symmetry of the systems was not taken into account. The weakly bound water chains are chosen for demonstrative purposes since the number of TEI is relatively small and the elongation cutoff procedure can be compared directly with the 'conventional' HF calculations. However, one should remember that the proper description of weakly bound systems requires post-HF methods and for these methods HF step is not time limiting one. The geometries of both model systems are shown in Fig. 3. For water chains three basis sets are employed: STO-3G [43], 6–31G [44], and 6–311G [45]. In polyglycine case, two basis set are used (STO-3G and 6–31G). All calculations are performed in cluster representation; methyl groups terminate both ends of the polyglycine clusters.

## Results and discussion

### Water chains

As we have described in the cutoff section, the elongation cutoff technique should substantially reduce the number of TEI that have to be computed. In Fig. 4, we have shown how the number of TEI increases with the size of the system. The circles corresponds to HF reference calculations while the squares to cutoff calculations. The lines are introduced for reason of clarity. The symbol *m*/*n* in the figure specifies the cutoff elongation procedure. It means that *m* residues were in the starting cluster and *n* residues were frozen and added in a time. Of course, the parameter *m* is connected with the size of the variational space and the difference *m*-*n* is a number of residues from the current chain that remains active in the next elongation step. Both parameters have direct connection with accuracy and CPU time. The bigger *m* is and the smaller *n* is, the more accurate are the calculations. However, the smaller *n* is, the longer the calculations. Parts a and b of Fig. 4 correspond to 6–31G and 6–311G basis sets, respectively. For 20 and

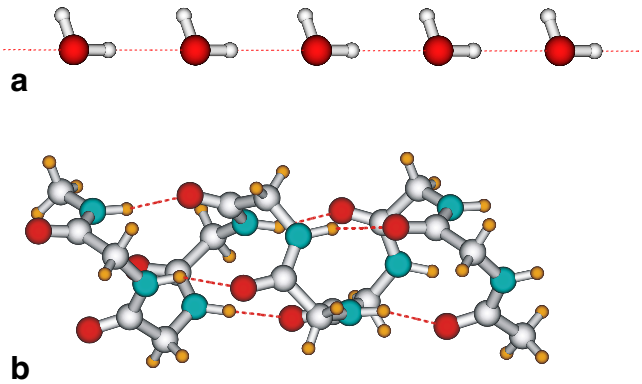


**Fig. 3** Structure of the discussed model systems: water chain (**a**) and α-helix conformer of polyglycine (**b**). Red broken lines indicate the hydrogen bonds

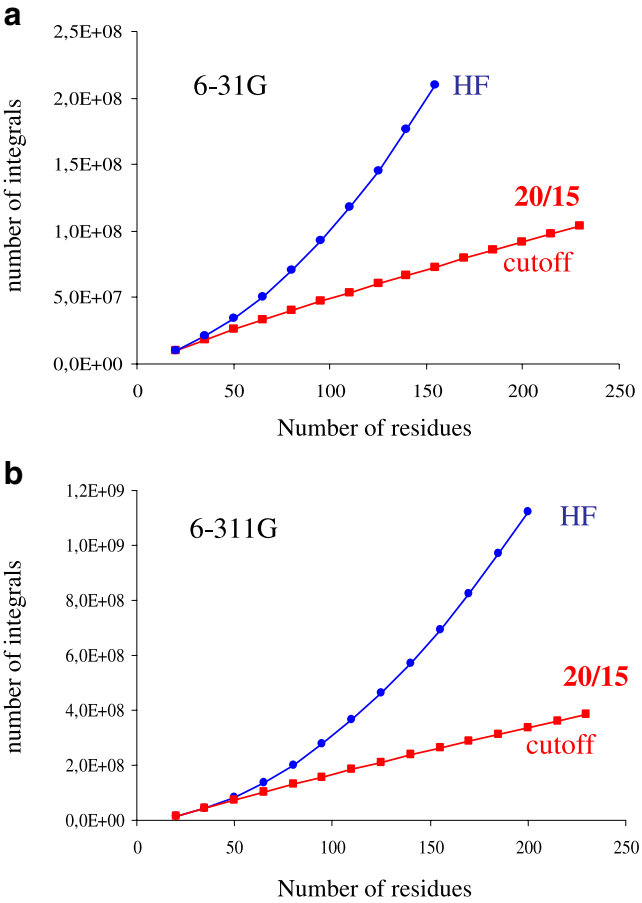


**Fig. 4** The number of two-electron integrals computed in each elongation cutoff (squares) and conventional HF (circles) steps for water chains at 6–31G (**a**) and 6–311G (**b**) levels of theory with the usage of disk-based algorithm

35 water molecules, the number of TEI in the elongation calculations is exactly the same as in the HF reference calculations. For 50 residues, the cutoff calculations are performed for the first time, so one can notice that the number of TEI is smaller than in the HF case. It is clear from the figure that the number of TEI in cutoff calculations increases linearly or sub-linearly. Dependence of the number of TEI on the system size is at least quadratic for HF calculations. Such kinds of dependencies suggests that cutoff calculations can be performed in 'conventional' calculations much longer than in HF calculations.

In Fig. 5, we compare cutoff and HF CPU times. Parts a, b and c of the figure correspond to STO-3G, 6–31G, and 6–311G basis sets, respectively. In the case of cutoff calculations two curves are plotted, one corresponding to step CPU time and second showing the total CPU time. The total CPU time in the *n*-th elongation step is a sum of the current and all the previous (*n*-1) CPU times: $\tau_{cutoff} = \sum_{i=1}^{n} \tau_i$. In all cases the step CPU time is much lower than the reference HF one. Nevertheless, the total CPU time is still quadratic and only the prefactor in the scaling relation

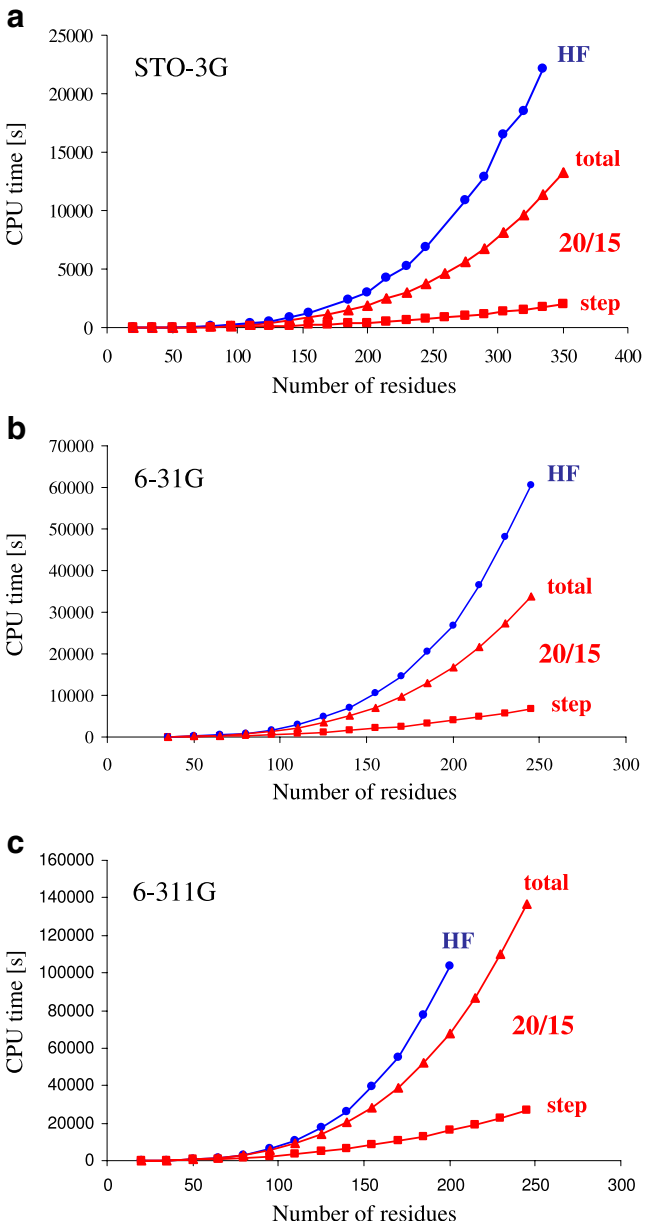


**Fig. 5** CPU timings for elongation cut-off (squares and triangles) and conventional (circles) calculations performed for water chains at STO-3G (**a**), 6–31G (**b**), and 6–311G (**c**) level of theory with the usage of disk-based algorithm. The elongation cutoff data include step (squares) and total (triangles) CPU time information

is reduced. This prefactor can be controlled by changing the size of the starting cluster and the type of partitioning. The CPU time savings can be seen in Fig. 6, where the ratio $\tau_{cutoff}/\tau_{HF}$ is plotted against the system size. At the beginning of the elongation process this ratio is higher than one for all the basis sets used in the calculations. It is connected with the additional costs we had to pay in the elongation cutoff calculations (MO localization and elongation procedures). The larger the basis set, the lower the value of this initial ratio. It is obvious since the additional time for elongation procedures is practically the same for all

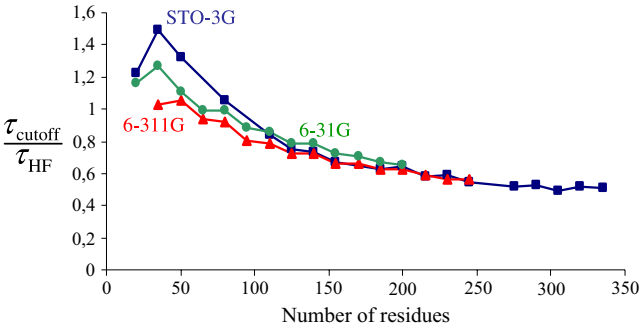


**Fig. 6** CPU time savings for elongation cutoff calculations performed with STO-3G (squares), 6–31G (circles), and 6–311G (triangles) basis sets

the basis sets while the CPU time for computing TEI and solving SCF equations increases much faster. The next observation is that all the curves have the same asymptotic behavior. Roughly speaking, we reduce the total CPU time by 40%. This can be attributed to the fact that even though we are constructing only a small subblock of the total Fock matrix, we have to compute all the integrals with at least two indices belonging to this subblock.

The only additional approximation in the elongation cutoff calculations, as compared to the HF reference calculations, is the reduction of the dimension of the variational space. In Fig. 7, we have shown how this approximation is reflected in the accuracy. It is clear from the figure that the elongation cutoff error, $\delta E = E_{cutoff} - E_{HF}$, is really very small. It is the smallest for STO-3G and the highest for 6–311G basis set. For all the basis sets the error is positive. It means that we didn't violate the orthogonality between frozen and active space LMOs. In other words, the elongation cutoff technique remains variational.

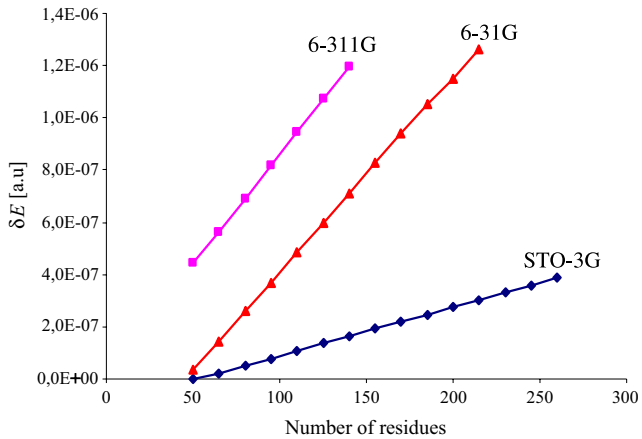


**Fig. 7** The error introduced by the elongation cutoff procedure for STO-3G (diamonds), 6–31G (triangles), and 6–311G (squares) basis sets

α-Helix conformer of polyglycine

The performance of the elongation cutoff technique for α-helix of polyglycine is shown in Fig. 8, where we have plotted step and total CPU time together with the reference HF CPU time. The polyglycine units are strongly coupled and the number of TEI quickly exceeds the disc capacity. For this reason, we have performed HF calculations in 'direct' mode. It means that all the required integrals were recalculated during SCF iterations. In order to reduce the CPU time of the reference HF calculations we apply the quantum fast multipole method (QFMM). The multipole method was not applied in the elongation cutoff calculation. If it was necessary, the total energy of a given cluster was computed in direct mode, while the whole SCF process was performed in the 'conventional' way. Similarly, as it was observed for water chains, the elongation cutoff step CPU time is lower than the reference HF/QFMM time for both basis sets. Now, the total CPU time is comparable to HF/QFMM one. However, the methodological consistency requires that the total CPU cutoff time should be compared to HF reference calculations performed without QFMM. Such a comparison is shown in inset to Fig. 8a. One can observe that the separation between HF and cutoff curves is huge and quickly increases with the system size. Such behavior explains why we have compared the elongation cutoff method with HF/QFMM one.

Taking into account that the normal elongation method (without cutoff) substantially reduces the CPU time in 'direct' calculations with QFMM included [34], it can be expected that after including QFMM into the cutoff technique, its 'direct' mode should be especially fast. The majority of integrals computed in the cutoff calculation are the long range Coulomb integrals for well separated Gaussian overlap distributions. Such integrals can be computed using QFMM. In addition, as long as, we have no need to compute the total energy, the QFMM memory requirements are not huge. We can remember information concerning multipoles belonging to cut region at the highest subdivision level (parent boxes). In addition, only a small subset of TEI which should be computed exactly, since their overlap charge distributions are not well separated, is needed in every elongation step. Only in final (termination) step all TEI should be computed. However, the SCF process is omitted since we know the system total density.

In comparison to water chains, the glycine units are strongly coupled in the helix. Therefore, the error introduced by the elongation method should be greater. We have not computed the error curves as previously. Instead, we have performed calculations for the biggest clusters. The

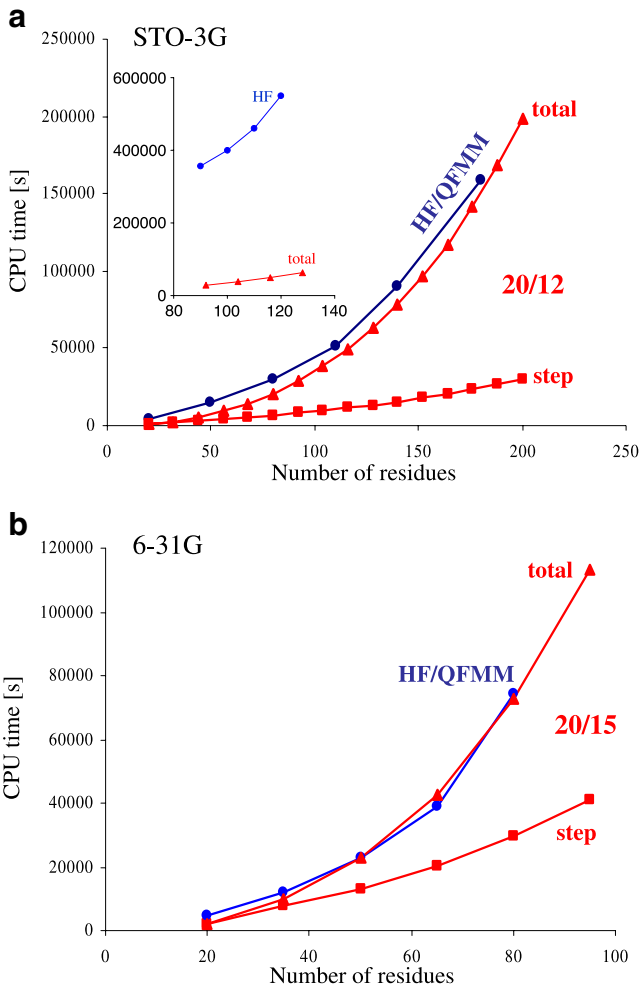


**Fig. 8** CPU timings for elongation cut-off (squares and triangles) and conventional (circles) calculations performed for polyglycine clusters at STO-3G (**a**) and 6–31G (**b**) level of theory. Cutoff calculations are done with the usage of disk-based algorithm. The reference HF calculations are performed at direct mode with QFMM. The elongation cutoff data include step (squares) and total (triangles) CPU timings. The inset in part a of the figure compares the elongation cutoff total CPU time with HF performed at direct mode without QFMM. The meaning of the axes is the same as in the main plot

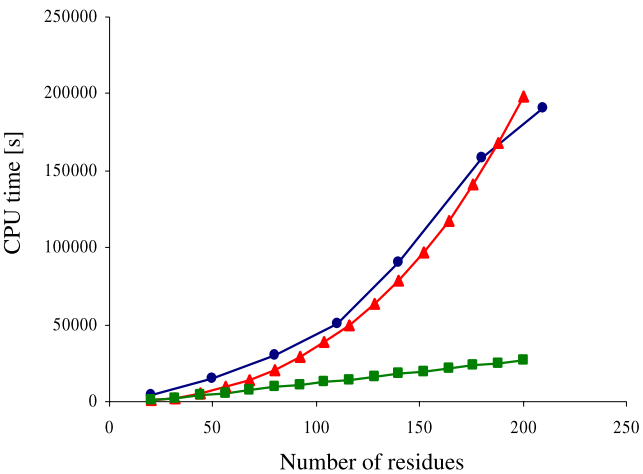


**Fig. 9** CPU timings for full and active space cutoff calculations for polyglycine clusters together with conventional HF calculations performed with STO-3G basis set

error for 6–31G basis set was lower than $1.2 \cdot 10^{-3}$ a.u. For the minimal STO-3G basis set was lower than $2.0 \cdot 10^{-4}$ a.u. The error can be controlled by the type of partitioning ($m/n$). By limiting $n$ to 5 (20/5) the accuracy is of the order $10^{-5}$.

Finally, we would like to demonstrate that after narrowing the area of interactions, the elongation technique is really linear. In Fig. 9, we have plotted the total CPU time as a function of the system size for the elongation cutoff calculation, in the case when interactions with cut fragments were excluded from computations. This dependence is linear (squares) and the correlation coefficient is almost one. One can also noticed that the CPU time is a few times lower than HF (circles) or full space cutoff (triangles) CPU time. The observed $\tau = \tau(N)$ dependence explains the linear scaling in majority of fragmentation techniques, since very often the interactions in these approaches are limited to a given molecular fragment or extend to the nearest neighboring fragments. It also suggests that we can introduce the interaction radius to the elongation cutoff calculation. In such a case, the dependence of the total CPU on the system size should be a straight line lying between both cutoff curves. The infinite radius corresponds to the full space cutoff calculations (triangles), while the zero radius corresponds to the active space cutoff calculations (squares). Another possibility to speed up the calculation is to use classical multipoles for distant interactions, e.g., Stone's multipole analysis [46]. Such interactions are one-electron in nature and are computed only once in every elongation cutoff step. By introducing the interaction radius and classical multipoles to the elongation cutoff technique, a linear scaling method with very small prefactor should be obtained. The QFMM step of HF method is linear, unfortunately, the prefactor of this relation is huge. A low prefactor is especially important for routine applications of computational methods to big molecular systems.

## Conclusions and future prospects

In this paper we have presented the elongation cutoff calculations for two model systems. The total CPU time and accuracy is discussed. It is shown that the number of TEI increases linearly with the system size. In spite of this, the 'conventional' type of calculations (integrals stored on a disc) can be extended to large systems. Even though the number of TEI increases linearly, the total CPU time *versus* the system size shows quadratic dependence. Nevertheless, the elongation cutoff method significantly reduces the prefactor in the quadratic scaling relation. It is argued that after introducing the interaction radii, a real linear scaling in the total CPU time can be obtained. Another way toward linear scaling is application of quantum fast multipole method to the elongation cutoff scheme in 'direct' type of calculations or combined 'conventional/direct' calculations. Taking into account that the overlap Gaussian distributions belonging to cut region are well separated from the active space distributions, such a scheme should be very efficient (time and memory requirements). We are planning to incorporate both mentioned techniques to the elongation cutoff method. The accuracy for weakly bound subsystems is higher than for strongly bonded subsystems. Nevertheless, it is satisfactory.

**Acknowledgements** Part of the calculation was performed at CYFRONET (MNiSW/SGI3700/UJ/161/2006 and MNiSW/SGI4700/UJ/061/2007). The work was supported by Polish Ministry of Science and Higher Education (Project No. 1486/B/H03/2007/33).

## References

1. White CA, Head-Gordon M (1994) J Chem Phys 101:6593–6605
2. White CA, Johnson BG, Gill PMW, Head-Gordon M, Chem (1996) Chem Phys Lett 253:268–278
3. Strain MC, Scuseria GE, Frisch MJ (1996) Science 271:51–53
4. Daniels AD, Scuseria GE (1999) J Chem Phys 110:1321–1328
5. Li X, Millam JM, Scuseria GE, Frisch MJ, Schlegel HB (2003) J Chem Phys 119:7651–7658
6. Watson MA, Salek P, Macak P, Helgaker T (2004) J Chem Phys 121:2915–2931
7. Gan CK, Tymczak CJ, Challacombe M (2004) J Chem Phys 121:6608–6614
8. Head-Gordon M, Maslen PE, White CA (1998) J Chem Phys 108:616–625
9. Constans P, Ayala PY, Scuseria GE (2000) J Chem Phys 113:10451–10458
10. Schütz M, Werner HJ (2001) J Chem Phys 114:661–681
11. Flocke N, Bartlett RJ (2003) J Chem Phys 118:5326–5334
12. Azhary AE, Rauhut G, Pulay P, Werner HJ (1998) J Chem Phys 108:5185–5193
13. Ayala PY, Scuseria GE (1999) J Chem Phys 110:3660–3671
14. Maslen PE, Lee MS, Head-Gordon M (2000) Chem Phys Lett 319:205–212
15. Pulay P, Saebø S, Wolinski K (2001) Chem Phys Lett 344:543–552
16. Yang W (1991) Phys Rev Lett 66:1438–1441
17. Yang W, Lee T-S (1995) J Chem Phys 103:5674–5678
18. Imamura A, Aoki Y, Maekawa K (1991) J Chem Phys 95:5419–5431
19. Aoki Y, Imamura A (1992) J Chem Phys 97:8432–8440
20. Imamura A, Aoki Y Nishimoto K, Yurihara Y, Nagao A (1994) Int J Quantum Chem 52:309–320
21. Mitani M, Aoki Y, Imamura A (1994) J Chem Phys 100:2346–2358
22. Aoki Y, Suhai S, Imamura A (1994) Int J Quantum Chem 52:267–280
23. Aoki Y, Suhai S, Imamura A (1994) J Chem Phys 101:10808–10823
24. Dixon SL, Merz KM Jr (1996) J Chem Phys 104:6643–6649
25. Dixon SL, Merz KM Jr (1997) J Chem Phys 107:879–893
26. Exner TE, Mezey PG (2003) J Comput Chem 24:1980–1986
27. Exner TE, Mezey PG (2004) J Phys Chem A 108:4301–4309
28. He X, Zhang JZH (2005) J Chem Phys 122:031103–031106
29. Chen X, Zhang Y, Zhang JZH (2005) J Chem Phys 122:184105
30. Li W, Li S (2005) J Chem Phys 122:194109–194115

31. Gu FL, Aoki Y, Korchowiec J, Imamura A, Kirtman B (2004) J Chem Phys 121:10385–10391
32. Korchowiec J, Gu FL, Aoki Y (2005) Int J Quantum Chem 105:875–882
33. Korchowiec J, Gu FL, Imamura A, Kirtman B, Aoki Y (2005) Int J Quantum Chem 102:785–794
34. Makowski M, Korchowiec J, Gu FL, Aoki Y (2006) J Comput Chem 27:1603–1619
35. Fedorov DG, Kitaura K (2004) J Chem Phys 120:6832–6840
36. Fedorov DG, Kitaura K (2004) Chem Phys Lett 389:129–134
37. Deev V, Collins MA (2005) J Chem Phys 122:154102–154111
38. Collins MA, Deev V (2006) J Chem Phys 125:104104–104115
39. Li S, Li W, Fang T (2005) J Am Chem Soc 127:7215–7226
40. Jiang N, Ma J, Jiang Y (2006) J Chem Phys 124:114112–114119
41. GAMESS, Version 14, Jan. 2003 (R2), Iowa State University
42. Schmidt MW, Baldridge KK, Boatz JA, Elbert ST, Gordon MS, Jensen JH, Koseki S, Matsunaga N, Nguyen KA, Su S, Windus TL, Dupuis M, Montgomery Jr JA (1993) J Comput Chem 14:1347–1363
43. Hehre WJ, Stewart RF, Pople JA (1967) J Chem Phys 51:2657–2664
44. Ditchfield R, Hehre WJ, Pople JA (1971) J Chem Phys 54:724–728
45. Krishnan R, Binkley JS, Seeger R, Pople JA (1980) J Chem Phys 72:650–654
46. Stone (1981) Chem Phys Lett 83:233–239